THE EUROPEAN
PHYSICAL JOURNAL PLUS

Regular Article

Propagation of angular momentum in charged pion decay and related processes

Bowen Wang[a]

School of Physics, Hangzhou Normal University, Hangzhou 311121, Zhejiang, China

Abstract There are confusions about angular momentum propagation in scattering or decay processes involving the transition between particle systems that appear to transform differently under Lorentz transformations. This paper provides an analysis of the transformation properties of the states and interactions for a few typical processes within the standard model of particle physics, and performs explicit calculations showing how angular momentum transfers in these processes. We shall show explicitly (a) how a state with zero angular momentum evolves via interactions mediated by a single vector boson of spin one, and (b) that angular momentum conservation is completely consistent with the calculation in quantum field theory. A discussion is also given about the phenomenological consequences of the theoretical results obtained in this study.

1 Introduction

Within the standard model (SM), the decay of a charged pion[1] (take π^- to be definite) into a lepton l^- and an anti-neutrino $\bar{\nu}_l$ occurs through weak interactions mediated by a W boson. This process is described in Fig. 1. The corresponding matrix element is

$$(2\pi)^4 \delta^{(4)}(k - k_1 - k_2) i \mathcal{M}(\pi^-(k) \to l^-(k_1)\bar{\nu}_l(k_2))$$
$$= -\frac{i\sqrt{2\pi\alpha}V_{ud}}{\sin\theta_W} \int d^4x \langle l^-(k_1)\bar{\nu}_l(k_2)| W_\mu^+(x) |0\rangle \times \langle 0| J_q^{\mu+}(x)|\pi^-(k)\rangle, \tag{1}$$

where α is the fine structure constant, V_{ud} the "ud" element of the quark mixing matrix, and θ_W the weak mixing angle. The definition of the amplitude $\mathcal{M}$ follows the convention of Ref. [1]. The pion and leptons are in "in" and "out" states respectively, and the fields between the states are all renormalized. The polarizations of the fermions[2] are not labeled explicitly. The $V - A$ quark current is defined by

$$J_q^{\mu+}(x) \equiv \overline{\Psi^u}(x)\gamma^\mu \frac{1 - \gamma^5}{2} \Psi^d(x). \tag{2}$$

Note that the decay occurs inevitably via the interaction term $W_\mu^+(x)J_q^{\mu+}(x)$, which is explicitly extracted in Eq. (1). The insertion of the vacuum states indicates then that the fields can only be contracted in such a way as to maintain a factorized form for the transition amplitude represented by the graph in Fig. 1. The first factor of the integrand in Eq. (1) gives the vertex function of two external fermions and an off-shell propagator [2, 3] with all order corrections including the self-energy graphs.[3] These are denoted by the blob in light grey in Fig. 1. The second factor has a simple tensor structure determined by the properties of the quark current and of the states under Lorentz transformations[4] and translations:

$$\langle 0|J_q^{\mu+}(x)|\pi^-(k)\rangle = \frac{i}{2}f_\pi k^\mu e^{-ik\cdot x}, \tag{3}$$

where f_π is the pion decay constant (in the convention of the particle data group [4]). It receives contributions from perturbative and non-perturbative interactions within the π^- induced by the quark current $J_q^{\mu+}(x)$. These interactions result in the decay of the pion and are represented by the blob in dark grey in Fig. 1.

Perturbative calculations can be done for the branching ratio $R_{e/\mu}^\pi \equiv \Gamma(\pi^- \to e^-\bar{\nu}_e)/\Gamma(\pi^- \to \mu^-\bar{\nu}_\mu)$, which is independent of f_π. The agreement between the SM prediction of $R_{e/\mu}^\pi$ (with radiative corrections) and measurements has reached a level within

---

[1] Or more generally, a charged pseudoscalar meson.

[2] We do not distinguish anti-fermions from fermions except where the distinction affects our discussion.

[3] Only half of the self-energy contribution should be included for the external lines in accord with the reduction of the S-matrix [2, 3].

[4] The Lorentz transformations (and Lorentz group) in this paper do not involve space inversion and time reversal operations.

---

[a] e-mail: bowenw@hznu.edu.cn (corresponding author)

Springer

Fig. 1 The decay of a charged pion into a lepton and an anti-neutrino: $\pi^- \to l^- \bar{\nu}_l$. The light blob represents purely perturbative interactions in the graph, while the dark blob also includes non-perturbative contributions
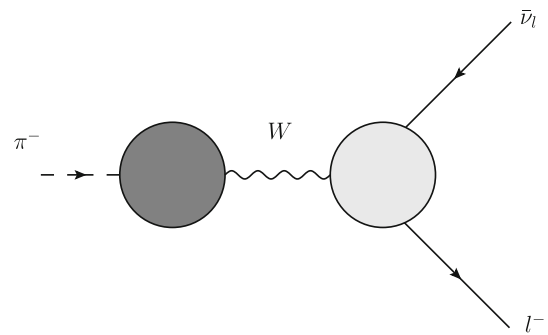
0.5%, and is limited by the accuracy of the experiment [5]. This provides a good precision test of the SM and perturbative calculations in quantum field theory. Furthermore, f_π can be calculated in lattice QCD (see Ref. [4], Table 72.1). It can also be extracted from experiments once the W decay subprocess (i.e., the first factor of the integrand on the r.h.s. of Eq. (1)) is computed (with parameters such as V_{ud} taken from other measurements). Comparison of results from both approaches shows an agreement at the percent level [4]. This is also the level of uncertainty of the Lattice QCD result.

On the other hand, measurements of the angular distributions of pion decay products in the pion rest frame were done in many early experiments. While most of them obtained isotropic results (e.g., Ref. [6–8]), small asymmetry were found in some of the studies (e.g., Ref. [9]). There are no reports of significant deviation from a uniform angular distribution in more recent experiments of pion decays [10, 11]. The limits for the sizes of possible Lorentz violating terms are set to the level of $10^{-5} \sim 10^{-4}$ relative to the SM terms [12–14].

It is a consensus that no anisotropic angular distributions can be deduced from the charged pion's SM decays, since the pion is a pseudoscalar and the interactions involved are all Lorentz invariant. Studies of possible Lorentz violating effects all seek to find the sources for Lorentz violation from extensions of the SM [12–16]. It may be conceptually confusing, however, that in the SM a spin-0 initial state propagates via a spin-1 vector boson, and remains isotropic before being measured. This is usually explained by noting that there is a longitudinal polarization mode of the massive vector boson that behaves like a scalar with 0 angular momentum [1, 17, 18]. In Ref. [19] the decay is considered as occuring via a spin-0 goldstone boson to avoid non-conservation of angular momentum. Nevertheless, it is still helpful to analyze the decay and other related processes using symmetry principles to show explicitly how angular momentum conservation manifests at the amplitude level.

In the following we shall first explore the rotational and Lorentz symmetries in production processes of a vector boson, and then illustrate the results based on symmetry considerations by simple tree level calculations. Consequences of the results in experiments will then be discussed. A summary and discussion of the results will be given at the end.

2 Angular momentum transfer in the production of a vector boson

It is helpful to first work out the angular momentum of a vector boson (vector current) created from a collision of two spin-1/2 fermions. This is somewhat more complicated than the case of charged pion decay, but it provides a richer picture as to how angular momentum is transferred between different parts of an amplitude. To make the discussion general, we start by considering the matrix element

$$\langle 0|J^\mu(x)|p_a, \lambda_a; p_b, \lambda_b\rangle = e^{-i(p_a+p_b)\cdot x}\langle 0|J^\mu(0)|p_a, \lambda_a; p_b, \lambda_b\rangle, \tag{4}$$

where J^μ denotes the SM current that tranforms like a vector, axial-vector, or a combination of them, e.g., $J^\mu = \overline{\Psi^e}\gamma^\mu\Psi^e$, $\overline{\Psi^e}\gamma^\mu\frac{1-\gamma^5}{2}\Psi^\nu$, etc. The momenta and helicities of the fermions are indicated in the state ket. This matrix element represents the all order contribution to the fermion-vector vertex shown in Fig. 2a (with the vector boson part excluded, as indicated by the vertical bar).

The initial state is made up of two fermions with definite momenta and helicities, as indicated in the state ket in Eq. (4). This is not an eigenstate of the angular momentum. To analyse the angular structure of the process, we expand the initial state as a combination of states with definite J, M, λ_a, λ_b, $\mathbf{P}^+ \equiv \mathbf{p}_a + \mathbf{p}_b$, and $E^+ \equiv \sqrt{\mathbf{p}_a^2 + m_a^2} + \sqrt{\mathbf{p}_b^2 + m_b^2}$ [20, 21]. J and M are respectively the quantum numbers for the total angular momentum of the fermions, and for its projection on the 3-axis in the center-of-mass (CM) frame of the fermions, in which the 3-direction is defined by the direction of the 3-momentum of a: $\mathbf{p} \equiv \mathbf{p}_a = -\mathbf{p}_b$. It is convenient to work in this CM frame and express the expansion as [20, 21]

$$|p_a, \lambda_a; p_b, \lambda_b\rangle = \sum_J C_J |J, M = \lambda_a - \lambda_b, \lambda_a, \lambda_b, |\mathbf{p}|\rangle, \tag{5}$$

Fig. 2 Vertices that produce a vector boson in the processes, **a** fermion-fermion scattering, and **b** decay (of e.g., $\pi^\pm$, Ψ, etc.). The light blob represents purely perturbative interactions in the graph, while the dark blob also includes non-perturbative contributions
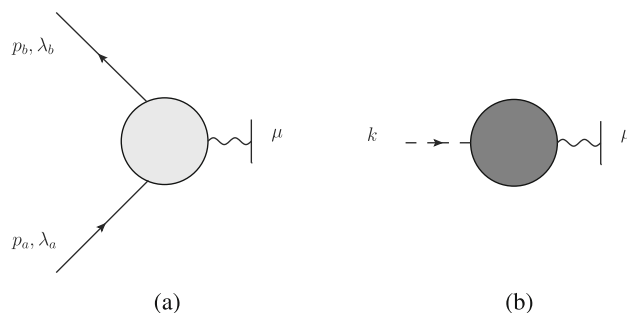
where $\mathbf{P}^+ = 0$ is suppressed, and E^+ is replaced by $|\mathbf{p}|$ in the states on the r.h.s. of Eq. (5). J runs over the integers 0, 1, ... There is no sum over M, because the 3-component of the angular momentum coincides with the difference of the helicities. For an anti-fermion, the physical spin in the direction of its momentum is opposite to its helicity, so an extra minus sign[5] is to be included in its helicity λ_a or λ_b when obtaining $M = \lambda_a - \lambda_b$. It is shown [20, 21] that $C_J = \sqrt{(2J+1)/(4\pi)}$ in order to be consistent with the normalization of the momentum and angular momentum eigenstates:

$$\langle p'_a, \lambda'_a; p'_b, \lambda'_b | p_a, \lambda_a; p_b, \lambda_b \rangle = (2\pi)^6 2E_a 2E_b \delta^3(\mathbf{p}'_a - \mathbf{p}_a)\delta^3(\mathbf{p}'_b - \mathbf{p}_b)\delta_{\lambda'_a \lambda_a}\delta_{\lambda'_b \lambda_b}, \tag{6}$$

$$\langle J', M', \lambda'_a, \lambda'_b, |\mathbf{p}'| | J, M, \lambda_a, \lambda_b, |\mathbf{p}| \rangle = (2\pi)^6 \frac{E^+}{|\mathbf{p}|}\delta^3(\mathbf{P}^{+\prime})\delta(E^{+\prime} - E^+)\delta_{J'J}\delta_{M'M}\delta_{\lambda'_a \lambda_a}\delta_{\lambda'_b \lambda_b}. \tag{7}$$

Note that Eq. (7) is expressed in the CM frame of $\mathbf{P}^+$, in which $\mathbf{P}^{+\prime}$ may be non-zero. For a non-zero $\mathbf{P}^{+\prime}$, Eq. (7) gives 0 irrespective of the 3-direction chosen in the CM frame of $\mathbf{P}^{+\prime}$ to define M'. Whereas if $\mathbf{P}^{+\prime} = \mathbf{P}^+ = 0$, both M and M' are defined with respect to the direction of $\mathbf{p}$. However, in Eq. (7), M and M' are not restricted to $M = \lambda_a - \lambda_b$ and $M' = \lambda'_a - \lambda'_b$, since the states are not restricted to those in the expansion in Eq. (5). The matrix element in Eq. (4) can also be expanded as

$$\langle 0 | J^\mu(0) | p_a, \lambda_a; p_b, \lambda_b \rangle = \sum_J C_J \langle 0 | J^\mu(0) | J, M = \lambda_a - \lambda_b, \lambda_a, \lambda_b, |\mathbf{p}| \rangle, \tag{8}$$

or, for a full process with the final state $|f\rangle$,

$$\langle f | p_a, \lambda_a; p_b, \lambda_b \rangle = \sum_J C_J \langle f | J, M = \lambda_a - \lambda_b, \lambda_a, \lambda_b, |\mathbf{p}| \rangle. \tag{9}$$

We are particularly interested in analysing the contribution to the matrix element in Eq. (8) from each value of J. A vanishing contribution from a specific J signifies that the propagation of this angular momentum eigenvalue is forbidden. To determine the allowed J values we should consider the transformation properties of both the operator J^μ and the state $|J, M = \lambda_a - \lambda_b, \lambda_a, \lambda_b, |\mathbf{p}|\rangle$. The angular momentum eigenstates with fixed J furnish an irreducible representation under the spatial rotation $R(\alpha, \beta, \gamma)$, which is a 3 by 3 matrix that rotates the spatial coordinates and is parameterized by the Euler angles α, β and γ:

$$U(R(\alpha, \beta, \gamma))|J, \lambda_a - \lambda_b, \lambda_a, \lambda_b, |\mathbf{p}|\rangle = \sum_{M'} \mathscr{D}^J_{M', \lambda_a - \lambda_b}(R(\alpha, \beta, \gamma))|J, M', \lambda_a, \lambda_b, |\mathbf{p}|\rangle. \tag{10}$$

Note that λ_a, λ_b, and $|\mathbf{p}|$ are invariant under rotations. M (on the l.h.s.) is fixed to $\lambda_a - \lambda_b$, but is changed by a rotation to M' (on the r.h.s.). The subscripts of the Wigner $\mathscr{D}$-matrix $\mathscr{D}^j_{m',m}$ (The explicit form can be found in e.g., [20, 22]) take the values $-J$, $-J+1$, ..., J. (All helicity values λ_a and λ_b are allowed as long as $-J \leq M = \lambda_a - \lambda_b \leq J$). The current operator $J^\mu(0)$ is a 4-vector that transforms according to

$$U(\Lambda)J^\mu(0)U^{-1}(\Lambda) = (\Lambda^{-1})^\mu_\nu J^\nu(0) \tag{11}$$

under an arbitrary Lorentz transformation Λ (The x dependence of J^μ is removed by translation in Eq. (4) so that the transformation of the current is simpler). On the r.h.s. of Eq. (11) μ and ν label respectively the row and column of the matrix Λ^{-1}. This is equivalent to the self-representation of the Lorentz group, which can be seen from the property for an arbitrary Lorentz transformation matrix Λ

$$g\Lambda g^{-1} = (\Lambda^{-1})^T, \tag{12}$$

$$g = g^{-1} = \mathrm{diag}\{1, -1, -1, -1\}. \tag{13}$$

Therefore $J^\mu(0)$ furnish a 4-dimensional irreducible representation of the Lorentz group. However, upon restriction to its spatial rotation subgroup $SO(3)$, the current operators are no longer irreducible. Clearly, J^0 is invariant under rotations, while J^1, J^2, and

---

[5] This extra minus sign is not to be confused with the minus sign in $M = \lambda_a - \lambda_b$.

J^3 are mixed. This reduces the 4 components to an $SO(3)$ singlet labeled by $J = 0$ and a triplet in the $SO(3)$ self-representation labeled by $J = 1$:

$$U(R)J^0(0)U^{-1}(R) = J^0(0)D_{0,0}^{J=0}(R), \quad D^{J=0}(R) = 1, \tag{14}$$

$$U(R)J^i(0)U^{-1}(R) = J^j(0)D_{j,i}^{J=1}(R), \quad D_{j,i}^{J=1}(R) = (R^{-1})_{i,j} = R_{j,i}, \quad i, j = 1, 2, 3. \tag{15}$$

As representations of the $SO(3)$ group with the same dimension are equivalent, the $D^{J=0}$ and $D^{J=1}$ matrices above are equivalent to the representations $\mathscr{D}^0$ and $\mathscr{D}^1$ in Eq. (10), respectively. Hence the only non-vanishing contribution in Eq. (8) is from $J = 0$ and $J = 1$ according to Wigner-Eckart theorem.[6] This is not exactly right because they could still vanish due to constraint from further symmetries (See Sect. 4 for an example), but at least all final states with $J \geq 2$ cannot be produced via a vector boson coupling to the vertex in Fig. 2a.

One may want to also investigate the transformation of $J^\mu(0)$ and $|J, M = \lambda - \lambda', \lambda, \lambda', |\mathbf{p}|\rangle$ under the full Lorentz group, rather than its subgroup. However, it is not straightforward to see the transformation law of the angular momentum eigenstates in this case, except that $|J = 0, M = \lambda - \lambda' = 0, \lambda, \lambda', |\mathbf{p}|\rangle$ will no longer be invariant (a boost changes the eigenvalues $\mathbf{P}^+$ and E^+).

The analysis above can be carried over immediately to the case of the charged pion decay (or more generally, charged pseudoscalar meson decay) via production of a W boson, as in Fig. 2b. The initial state pion is a pseudoscalar with $J = M = 0$, and the amplitude $\langle 0|J_q^{\mu+}(x)|\pi^-(k)\rangle$ in Eq. (3) is non-zero from the same reasoning as given above of the $J = 0$ contribution being non-zero in two fermion scatterings.

3 Amplitudes with angular momentum eigenstates

Now we derive formulae for practical calculations of the amplitudes on the r.h.s. of Eq. (9). The spatial part of p_a in Eq. (5) can be rotated by $R(\phi, \theta, 0)$ to a direction determined by the azimuthal angle ϕ and polar angle θ, with respect to the original axes. Denoting the initial state under this rotation by

$$|\phi, \theta, \lambda_a, \lambda_b, |\mathbf{p}|\rangle \equiv U(R(\phi, \theta, 0))|p_a, \lambda_a; p_b, \lambda_b\rangle = |R(\phi, \theta, 0)p_a, \lambda_a; R(\phi, \theta, 0)p_b, \lambda_b\rangle, \tag{16}$$

$$|p_a, \lambda_a; p_b, \lambda_b\rangle = |\phi = 0, \theta = 0, \lambda_a, \lambda_b, |\mathbf{p}|\rangle, \tag{17}$$

we obtain the expansion of the momentum eigenstates in an arbitrary direction by applying the rotation on Eq. (5):

$$|\phi, \theta, \lambda_a, \lambda_b, |\mathbf{p}|\rangle = \sum_{J,M} C_J \mathscr{D}_{M,\lambda_a-\lambda_b}^J(R(\phi, \theta, 0))|J, M, \lambda_a, \lambda_b, |\mathbf{p}|\rangle. \tag{18}$$

The inverse expansion can be obtained using the properties of the $\mathscr{D}$-matrices:

$$|J, M, \lambda_a, \lambda_b, |\mathbf{p}|\rangle = C_J \int_0^{2\pi} d\phi \int_0^\pi d\theta \sin\theta \, \mathscr{D}_{M,\lambda_a-\lambda_b}^{J*}(R(\phi, \theta, 0))|\phi, \theta, \lambda_a, \lambda_b, |\mathbf{p}|\rangle. \tag{19}$$

This can be used to compute perturbatively the amplitude for the production of a vector boson from a state with a particular J:

$$\langle 0|J^\mu(0)|J, M, \lambda_a, \lambda_b, |\mathbf{p}|\rangle = C_J \int_0^{2\pi} d\phi \int_0^\pi d\theta \sin\theta \, \mathscr{D}_{M,\lambda_a-\lambda_b}^{J*}(R(\phi, \theta, 0))\langle 0|J^\mu(0)|\phi, \theta, \lambda_a, \lambda_b, |\mathbf{p}|\rangle, \tag{20}$$

or, for a full process with the final state $|f\rangle$,

$$\langle f|J, M, \lambda_a, \lambda_b, |\mathbf{p}|\rangle = C_J \int_0^{2\pi} d\phi \int_0^\pi d\theta \sin\theta \, \mathscr{D}_{M,\lambda_a-\lambda_b}^{J*}(R(\phi, \theta, 0))\langle f|\phi, \theta, \lambda_a, \lambda_b, |\mathbf{p}|\rangle. \tag{21}$$

The Feynman rules for the momentum eigenstates on the r.h.s. of Eqs. (20), (21) are well known. In the following we shall compute a few simple processes to show the propagation of J values.

4 Example processes

We consider 2 to 2 tree level fermion scattering processes in s-channel mediated by a vector boson. The two processes in Fig. 3 will be treated in sequence. In these calculations, we would like to see explicitly the contribution from the $J = 0$ and $J = 1$ eigenstates, in accord with the generic result obtained in Sect. 2. Therefore the initial and final state fermions are taken to have definite helicities such that the angular structure of the processes are easily revealed. Specifically, we require that the two fermions in the initial state have the opposite spin components along the direction of the incoming beams. This is necessary to ensure that the $J = 0$ partial

---

[6] The rule of adding two angular momenta dictates that $J^\mu(0)$ and $|J, M = \lambda - \lambda', \lambda, \lambda', |\mathbf{p}|\rangle$ must be in equivalent representations in order to be combined by Clebsch-Gordon coefficients to form a singlet under rotations.
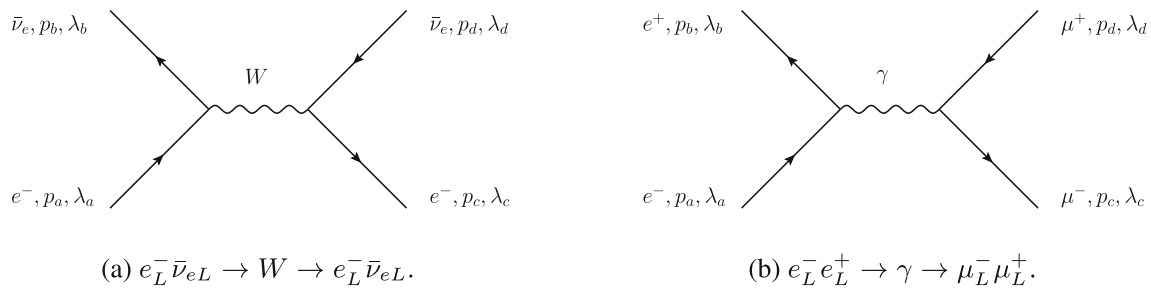
Fig. 3 Example 2 to 2 processes at tree level with the production and decay of a vector boson, where the fermion polarizations are defined by their helicities given in the main text

wave is non-zero in the expansion of the momentum eigenstates in Eq. (5). In contrast, if the fermions have the same spin along the beam, then the total spin of the system is $S = 1$, which cannot be canceled by the orbital angular momentum to give $J = 0$ because the orbital angular momentum is perpendicular to the beam direction. In this case, the partial wave expansion only contains terms with $J \geq 1$.

4.1 $e_L^-(p_a)\bar{\nu}_{eL}(p_b) \to W \to e_L^-(p_c)\bar{\nu}_{eL}(p_d)$

Here the subscript "L" for all the four fermions refers to the helicity configuration $\lambda_a = -\lambda_b = \lambda_c = -\lambda_d = -1$, rather than definite chiralities. In other words, we use "L" and "R" to describe the relation between the direction of a particle's physical spin and the direction in which it moves. This choice of polarizations is not contradicting to the fact that the anti-neutrino can only be right-handed in chirality, as long as it is a massive particle. Recall that when obtaining $M = \lambda_a - \lambda_b$ we give an extra minus sign to λ_b for the anti-neutrino, so that in this case $M = 0$ instead of -2. In the massless limit, the helicity and chirality eigenstates coincide, but this amplitude vanishes by helicity conservation. However, we shall keep the fermion masses so that the $J = 0$ mode is allowed, as will be seen below. Recall that we are examining the propagation of each J-mode in principle rather than evaluating the practical importance of the contribution from each J (which will be discussed in Sect. 5).

The initial momenta are

$$p_a = (E_a, 0, 0, p), \quad E_a = \sqrt{m_a^2 + p^2}, \tag{22}$$

$$p_b = (E_b, 0, 0, -p), \quad E_b = \sqrt{m_b^2 + p^2}, \tag{23}$$

where $m_a \equiv m_e$, and $m_b \equiv m_{\nu_e}$. The tree level vertex for the subprocess $e_L^-(p_a)\bar{\nu}_{Le}(p_b) \to W$ is (excluding the W propagator and an overall factor $-i\sqrt{2\pi\alpha}/\sin\theta_W$ at the vertex)

$$V^\mu(e_L^-(p_a)\bar{\nu}_{eL}(p_b) \to W) = \langle 0|J^\mu(0)|p_a, \lambda_a; p_b, \lambda_b\rangle_{\text{tree}} = \bar{v}^{\lambda_b}(p_b)\gamma^\mu \frac{1-\gamma^5}{2} u^{\lambda_a}(p_a), \tag{24}$$

where $J^\mu(0) = \overline{\Psi^{\nu_e}}\gamma^\mu \frac{1-\gamma_5}{2} \Psi^e$, and the particle species are omitted in the states and spinors. Here we follow the method in Ref. [1] to compute the amplitude for polarized states and employ the Weyl representation for the Dirac γ-matrices:

$$\gamma^0 = \begin{pmatrix} 0 & 1 \\ 1 & 0 \end{pmatrix}, \quad \gamma^i = \begin{pmatrix} 0 & \sigma_i \\ -\sigma_i & 0 \end{pmatrix}, \quad \gamma^5 = \begin{pmatrix} -1 & 0 \\ 0 & 1 \end{pmatrix}, \tag{25}$$

in which each element is a 2 by 2 matrix and σ_i are the Pauli matrices. The corresponding spinors for the spin-up electron and spin-down anti-neutrino (both with respect to the 3-direction) are

$$[u^{\lambda_a}(p_a)]^T = (0, \sqrt{E_a + p}, 0, \sqrt{E_a - p}), \tag{26}$$

$$[v^{\lambda_b}(p_b)]^T = (0, \sqrt{E_b - p}, 0, \sqrt{E_b + p}). \tag{27}$$

Inserting these expressions into Eq. (24) gives

$$V^\mu(e_L^-(p_a)\bar{\nu}_{eL}(p_b) \to W) = \sqrt{(E_b - p)(E_a + p)}(1, 0, 0, 1). \tag{28}$$

The vertex for $W \to e_L^-(p_c)\bar{\nu}_{eL}(p_d)$ is

$$V^\mu(W \to e_L^-(p_c)\bar{\nu}_{eL}(p_d)) = \bar{u}^{\lambda_c}(p_c)\gamma^\mu \frac{1-\gamma^5}{2} v^{\lambda_d}(p_d) = \left[\bar{v}^{\lambda_d}(p_d)\gamma^\mu \frac{1-\gamma^5}{2} u^{\lambda_c}(p_c)\right]^*. \tag{29}$$

The term in the square brackets is of the same form as in Eq. (24), except the momenta $\mathbf{p}_a = -\mathbf{p}_b$ are rotated from the 3-direction to $\mathbf{p}_c = -\mathbf{p}_d$. This term must be a 4-vector that transforms the same way as p_a and p_b under the rotation $\Lambda(R)$ that rotates them to p_c and p_d. This simply follows from the transformation of the vertex function

$$
\begin{aligned}
& \langle 0|J^\mu(0)|p_c, \lambda_a; p_d, \lambda_b\rangle \\
& = \langle 0|U(\Lambda(R))U^{-1}(\Lambda(R))J^\mu(0)U(\Lambda(R))U^{-1}(\Lambda(R))|p_c, \lambda_a; p_d, \lambda_b\rangle, \\
& = \Lambda(R)^\mu_\nu \langle 0|J^\nu(0)|\Lambda^{-1}(R)p_c, \lambda_a; \Lambda^{-1}(R)p_d, \lambda_b\rangle \\
& = \Lambda(R)^\mu_\nu \langle 0|J^\nu(0)|p_a, \lambda_a; p_b, \lambda_b\rangle,
\end{aligned}
\tag{30}
$$

which gives[7] immediately at tree level

$$
V^\mu(W \to e_L^-(p_c)\bar{\nu}_{eL}(p_d)) = \left[\Lambda(R)^\mu_\nu V^\mu(e_L^-(p_a)\bar{\nu}_{eL}(p_b) \to W)\right]^* = \sqrt{(E_b - p)(E_a + p)}(1, \mathbf{p}_c/p),
\tag{31}
$$

where $E_a = E_c$ and $E_b = E_d$.

Now restore the couplings (and other overall factors) at the vertices and contract with the W propagator in unitary gauge[8]

$$
\frac{-i}{q^2 - M_W^2}\left(g_{\mu\nu} - \frac{q_\mu q_\nu}{M_W^2}\right)
$$
$$
(q \equiv p_a + p_b)
\tag{32}
$$

to get the amplitude for the full process

$$
\begin{aligned}
& \mathcal{M}(e_L^-(p_a)\bar{\nu}_{eL}(p_b) \to W \to e_L^-(p_c)\bar{\nu}_{eL}(p_d)) \\
& = \frac{2\pi\alpha}{\sin^2\theta_W} \frac{(E_b - p)(E_a + p)}{(E_a + E_b)^2 - M_W^2}\left[1 - \frac{(E_a + E_b)^2}{M_W^2} - \cos\theta\right],
\end{aligned}
\tag{33}
$$

where M_W is the mass of the W boson. The dependence of the result on the external momenta is only through the angle θ between the initial and final fermion beams.

It is straightforward to compute the amplitude with an angular momentum eigenstate using Eq. (21), in the form

$$
\begin{aligned}
& \langle \phi, \theta, \lambda_c = \lambda_a, \lambda_d = \lambda_b, p|J, M, \lambda_a, \lambda_b, p\rangle \\
& = C_J \int_0^{2\pi} d\phi' \int_0^\pi d\theta' \sin\theta' \mathscr{D}^{J*}_{M,\lambda_a-\lambda_b}(R(\phi', \theta', 0)) \langle \phi, \theta, \lambda_c = \lambda_a, \lambda_d = \lambda_b, p|\phi', \theta', \lambda_a, \lambda_b, p\rangle.
\end{aligned}
\tag{34}
$$

The matrix element on the r.h.s. of Eq (34) is computed with the initial and final states

$$
|i\rangle \equiv |p_a', \lambda_a; p_b', \lambda_b\rangle = |\phi', \theta', \lambda_a, \lambda_b, |\mathbf{p}_a'| = p\rangle,
\tag{35}
$$

$$
|f\rangle \equiv |p_c, \lambda_c; p_d, \lambda_d\rangle = |\phi, \theta, \lambda_c = \lambda_a, \lambda_d = \lambda_b, |\mathbf{p}_c| = p\rangle,
\tag{36}
$$

$$
\langle f|i\rangle_{\text{tree}} = \langle p_c, \lambda_c; p_d, \lambda_d|p_a', \lambda_a; p_b', \lambda_b\rangle_{\text{tree}} = N_{ab}\left[1 - \frac{(E_a + E_b)^2}{M_W^2} - \cos\theta_{ac}\right],
\tag{37}
$$

where on the r.h.s. of Eq. (37) (and below), we suppress the factor $i(2\pi)^4$ and the delta function that implements the overall momentum conservation. N_{ab} represents the coefficient in Eq. (33) multiplying the square bracket, and θ_{ac} is the angle between $\mathbf{p}_a'$ and $\mathbf{p}_c$:

$$
\cos\theta_{ac} = \sin\theta \sin\theta' \cos(\phi - \phi') + \cos\theta \cos\theta'.
\tag{38}
$$

There is no contradiction between Eq. (37) and Eq. (6), because Eq. (37) is a product of "in" and "out" states that makes a transition amplitude in the presence of interactions, while Eq. (6) is a normalization condition when both states are "in", "out", or free states. We do not label these states with "in", "out", or "free" since they can be distinguished by context.

Inserting the explicit expressions for the $\mathscr{D}$-matrices [20, 22], the angular integration of Eq. (34) can be trivially performed to give

$$
\langle \phi, \theta, \lambda_c = \lambda_a, \lambda_d = \lambda_b, p|J, M, \lambda_a, \lambda_b, p\rangle_{\text{tree}} = N_{ab} \times
\begin{cases}
-\sqrt{\dfrac{4\pi}{3}}\cos\theta, & \text{for } J = 1, M = 0, \\[2ex]
\sqrt{4\pi}\left[1 - \dfrac{(E_a + E_b)^2}{M_W^2}\right], & \text{for } J = 0, M = 0.
\end{cases}
\tag{39}
$$

---

[7] The tensor structure on the r.h.s. of Eq. (3) can be deduced in a similar way.

[8] We would like to show that the propagation of zero angular momentum is possible without resorting to the unphysical Goldstone boson.

Hence, both $J = 0$ and $J = 1$ partial waves contribute to the amplitude Eq. (33).[9] Indeed, plugging the result of Eq. (39) into the expansion Eq. (9) reproduces Eq. (33) immediately. Note the $J \geq 2$ contribution vanishes. This can be seen from the form of the terms on the r.h.s. of Eq. (37). Those terms proportional to 1 and $\cos \theta'$ can be expressed by the matrix elements $\mathscr{D}_{00}^{J=0}$ and $\mathscr{D}_{00}^{J=1}$, which are orthogonal to the $\mathscr{D}_{00}^{J*}$ with $J \geq 2$ in the integration in Eq. (34). The other terms are proportional to eigher $\cos \phi'$ or $\sin \phi'$, which vanish after the integral over ϕ'. This is consistent with our general argument that states with $J \geq 2$ transform differently from the transformation of the current under rotations. Note that the argument was made for the vertex in Fig. 2a, with all order contributions. However, the vanishing of the vertex must be order by order since the perturbation series is zero for arbitrary values of the coupling constants involved in the interactions.

4.2 $e_L^-(p_a)e_L^+(p_b) \to \gamma \to \mu_L^-(p_c)\mu_L^+(p_d)$

A calculation similar to the one carried out above gives

$$\mathcal{M}(e_L^-(p_a)e_L^+(p_b) \to \gamma \to \mu_L^-(p_c)\mu_L^+(p_d)) = -\frac{4\pi\alpha m_a m_c}{E_a^2}\cos\theta, \tag{40}$$

where $m_a = m_e$ and $m_c = m_\mu$. In place of Eq. (39) we have

$$\langle \phi, \theta, \lambda_c = \lambda_a, \lambda_d = \lambda_b, p | J, M, \lambda_a, \lambda_b, p \rangle_{\text{tree}} = N_{ab} \times \begin{cases} -\sqrt{\dfrac{4\pi}{3}}\cos\theta, & \text{for } J = 1, M = 0, \\ 0, & \text{for } J = 0, M = 0, \end{cases} \tag{41}$$

where now N_{ab} stands for the factor multiplying $-\cos\theta$ in Eq. (40). This result shows that only the $J = 1$ mode contributes to the angular distribution of the final state, which by itself reproduces Eq. (40). The amplitudes with $J \geq 2$ are zero by the similar arguments given above. The new feature compared to the e^--$\bar{\nu}_e$ scattering is the vanishing of the $J = 0$ result, which is not a coincidence and has a deeper origin.

To see this we note that a positronium state with definite spin S and orbital angular momentum L is an eigenstate of the charge conjugation operator C, with the eigenvalue $\eta_C = (-1)^{L+S}$ [17, 23]. This property can be carried over to analyzing our process with an unbounded electron-positron pair. The state $|J, M, \lambda_a, \lambda_b, p\rangle$ with $J = M = 0$ has a definite J rather than L or S. However, the rule of adding two angular momenta requires that $J = 0$ can only be obtained by combining states with definite L and S that satisfy $L = S$. For all these states, $(-1)^{L+S} = 1$, and $|J = 0, M = 0\rangle$ is therefore a state that is even under charge conjugation:

$$C|J = 0, M = 0\rangle = |J = 0, M = 0\rangle, \tag{42}$$

where the quantum numbers other than J and M are suppressed in the state. Since the electromagnetic current is C-odd, we have

$$\begin{aligned} \langle 0|J^\mu(0)|J = 0, M = 0\rangle &= \langle 0|C^{-1}CJ^\mu(0)C^{-1}C|J = 0, M = 0\rangle \\ &= -\langle 0|J^\mu(0)|J = 0, M = 0\rangle \\ &= 0, \end{aligned} \tag{43}$$

which merely reflects the fact that J^μ and $|J = 0, M = 0\rangle$ belong to different representations of the charge conjugation operation (one C-even and the other C-odd). So the $J = 0$ mode does vanish.[10] Apparently, this argument cannot be applied to the case of e^--$\bar{\nu}_e$ scattering or charged pion decay, because the initial state of either process has a net electric charge that is reversed by C, and is therefore not an eigenstate of C. The initial state must then have a non-zero projection onto the C-odd space of the states, such that the amplitude with the current is not restricted to zero by charge conjugation.

5 Phenomenology

Given a non-zero $J = 0$ mode carried by a massive gauge boson in processes from previous sections, the immediate question about the role of this mode arises when determining the spin of the vector boson from experiments. For instance, the spin of the W boson was determined by measurement of the angular distribution of the electrons or positrons from the decay $W \to e\nu_e$ in the experiment carried out by the UA1 collaboration [24–26], in which W bosons were produced via Drell-Yan like processes in proton-antiproton collisions. The measured unpolarized[11] distribution is consistent with the shape $(1 + \cos\theta)^2$, where θ is the angle between the

---

[9] The smallness of the neutrino mass m_b makes the factor $E_b - p$ close to zero in the expression for the amplitude (which does not affect our arguments of course). If one chooses to compute alternatively the amplitude for the same process but with all external fermions right-handed, a factor $E_a - p$ will appear instead of $E_b - p$, and the non-zero contribution is still from $J = 0$ and $J = 1$.

[10] The result here and in Sect. 2 are obtained for the vertex functions. However, as we are focusing on s-channel graphs with a vector boson, these vertices are parts of the amplitudes. Furthermore, even though the contribution from J^μ, with $\mu = 1, 2$, or 3 is also zero by rotational invariance of the states, this does not ensure they are zero outside the CM frame of the electron-positron pair (where the rotational invariance of the initial state is lost. See Eq. (3) for a similar instance, where the spatial components of the matrix element is non-zero outside the pion rest frame.), unless the contribution from J^0 is also zero.

[11] The filtering of various polarization combinations is only done through the nature of the $V - A$ interactions.

directions of the electron (positron) and the proton (antiproton) in the rest frame of the W boson. The shape of the distribution can be traced back to the Wigner $\mathscr{D}$-matrix $\mathscr{D}^{1*}_{1,1}(R(\phi, \theta, 0)) = e^{-i\phi}(1 + \cos\theta)/2$. It shows that the W boson is produced in a state with $J = M = 1$.

The scalar mode[12] of the W boson contributes an isotropic term to the distribution of the decay product (see Eq. 39). This would in principle distort the distribution deduced from the vector mode of the W. However, the $V - A$ form only allows left-handed fermions and right-handed antifermions to participate in the interaction in the massless limit, in which case the propagation of the scalar mode is forbidden. In fact, it is straightforward to show that a fermion (antifermion) with a right-handed (left-handed) spin would introduce a factor $\sqrt{E - |\mathbf{p}|} = m/\sqrt{E + |\mathbf{p}|}$ to the scattering amplitude, where E, $\mathbf{p}$, and m are the energy, 3-momentum, and mass of the fermion (antifermion) (See Eqs. (28) and (31) for instance). If $m \ll E$, this gives a suppression factor $m/(2E)$ (known as helicity suppression) relative to the amplitude that is not suppressed (e.g., the one proportional to $\mathscr{D}^{1}_{1,1}(R(\phi, \theta, 0))$ above). Here E is of the order of the parton level CM energy for the scattering.

For an estimate with the UA1 experiment we could take $E \sim 100$ GeV, and consider the scalar mode that propagates via the process $d_R \bar{u}_R \to W \to \mu^-_R \bar{\nu}_{\mu R}$ (The process with left handed spins is much smaller since the final state suppression factor is from the mass of the neutrino rather than from that of the muon. Also we consider the muon instead of the electron in the final state since it has a larger mass). The suppression factor at the cross section level is $\sim \mathcal{O}((\frac{m_d m_\mu}{4E^2})^2) \sim 10^{-16}$. This is far too small to be observed. The statistical uncertainty of the measured angular distribution in the UA1 experiment is as large as 50%. For total cross section and forward-backward asymmetry observables, the accuracy improves to $\sim 10\%$. More recent measurements at the Fermilab Tevatron [27, 28] and the LHC [29, 30] reached a percent or even per-mille level accuracy, but are still far from being sensitive to the mass-suppressed modes.

To further reduce the mass-suppression effect on the scalar mode, we might consider the s-channel single top production, so that the final state suppression factor comes from the top quark mass. However, not much could be done about the initial state. Even if we consider the "sea-sea" contribution to the production of the W boson and take the charm quark from an incoming beam, we get a factor $\sim \mathcal{O}((\frac{m_c m_t}{4E^2})^2) \sim 10^{-6}$, where $E \sim 300$ GeV for the Tevatron experiment. This will further be suppressed by the sea quark distributions. Also the identification of the top final state is much more difficult than the leptonic decay product of the W [31–34].

At this point it appears hopeless to probe the $J = 0$ state of a massive vector boson produced via Drell-Yan (like) processes.[13] It is out of the scope of this study to perform a scan of processes, but here we leave the possibility open that this scalar state could manifest in some other production modes of the vector bosons, in addition to the decay processes of e.g., the charged pions.

6 Summary and discussion

In this study, we analyze the propagation of angular momentum via a vector boson in several processes by expanding the initial states into a superposition of angular momentum eigenstates of the system. Through a general discussion based on symmetry principles and two practical calculations, we are able to show that both the singlet ($J = 0$) and triplet ($J = 1$) representations of the rotation group can be transferred to the final state via an intermediate vector boson, unless constraints from further symmetries are present to forbid it. However, we have shown that the scalar state of a massive vector boson is produced with an extremely small rate that it has no impact on existing experiments at hadron colliders. The decays of several spin-zero particles, such as the charged pions, are the only obvious phenomena we have found related with the scalar state of gauge bosons.

The crucial point to understand the $J = 0$ case is that an initial state that is invariant under spatial rotations is not a singlet under a generic Lorentz transformation. The $J = 0$ state can be changed by boosts in any direction and gives a non-zero matrix element for producing a Lorentz vector current to which a massive gauge boson couples. Hence there is no Lorentz violation in the production of an off-shell gauge boson from such a state via interactions that are Lorentz invariant. The spin of a vector boson as a virtual particle has to be measured via its decay product and is not necessarily equal to its spin as a free field.

On the other hand, an on-shell vector boson should only be in a state with spin 1, and this should also be reflected at the amplitude level. We have shown that a state with $J = M = 0$ can propagate though the $\mu = 0$ component of a vector current, as appears in Eq. (8). However, this fact alone does not ensure the full amplitude with a $J = M = 0$ initial state is none zero, since the initial vertex function will be contracted with the rest part of the amplitude via the propagator of a gauge boson. For instance, we may think of the decay amplitude for $\pi^- \to l^- \bar{\nu}_l$ at leading order. After accounting for Eq. (3), the amplitude takes the form

$$\mathcal{M}(\pi^-(k) \to l^-(k_1)\bar{\nu}_l(k_2)) \sim k^\mu \frac{-g_{\mu\nu} + \frac{k_\mu k_\nu}{M_W^2}}{k^2 - M_W^2 + i\epsilon} \bar{u}(k_1)\gamma^\nu \frac{1 - \gamma^5}{2} v(k_2) \tag{44}$$

---

[12] The scalar and vector modes in this section refer to the behaviors of the states under spatial rotations.

[13] Note that not only the scalar mode, but also the one with $J = 1$, $M = 0$ (see Eq. 39) is suppressed. However, this latter mode also propagates via a final state with no suppression factor, e.g., $d_R \bar{u}_R \to W \to \mu^-_L \bar{\nu}_{\mu R}$. (The suppression factor is only from the initial state.) A similar estimate gives a somewhat larger result for this process compared with the scalar mode. But the improvement is still very limited compared to the uncertainties of the measurements.

where the tensor structure of the propagator in unitary gauge is obtained on the W mass shell by summing over three physical polarization vectors of the W boson

$$\sum_{\epsilon_\mu k^\mu = 0} \epsilon_\mu \epsilon_\nu^* = -g_{\mu\nu} + \frac{k_\mu k_\nu}{M_W^2}. \tag{45}$$

These polarization vectors are purely spatial in the W rest frame and make an $SO(3)$ triplet under rotations. Therefore the contraction of the propagator with k^μ (whose spatial components are all zero) in Eq. (44) gives

$$k^\mu \frac{-g_{\mu\nu} + \frac{k_\mu k_\nu}{M_W^2}}{k^2 - M_W^2 + i\epsilon} = \frac{k_\nu}{M_W^2} \frac{k^2 - M_W^2}{k^2 - M_W^2 + i\epsilon} = \begin{cases} 0, & k^2 = M_W^2, \\ k_\nu/M_W^2, & k^2 \neq M_W^2. \end{cases} \tag{46}$$

Of course, experimentally the pion mass m_{π^-} is much smaller than M_W. But as M_W is a free parameter of the SM, we allow k^2 to get on the W mass shell (i.e., $m_{\pi^-} = M_W$) for the purpose of checking the consistency of the calculation. The infinitesimal imaginary part of the denominator in Eq. (46) then ensures that the contraction is zero. This structure of contraction persists in loop corrections of the decay amplitude to all orders. Therefore an on-shell W boson indeed forbids the propagation of a $J = 0$ state. In the off-shell case, however, the state of the W boson cannot be described by the polarization vectors in Eq. (45) that furnish a $\mathscr{D}^1$ representation of the rotation group, and hence allows for a non-zero decay rate. This discontinuous transition of the decay amplitude to zero at the W mass shell shows clearly the consistency of SM dynamics with angular momentum conservation.[14]

Data availability statement There is no data associated with this study.

References

1. M.E. Peskin, D.V. Schroeder, *An Introduction to Quantum Field Theory* (Addison-Wesley, Reading, 2008)
2. S. Weinberg, *The Quantum Theory of Fields. Foundations*, vol. 1 (Cambridge University Press, Cambridge, 2005). https://doi.org/10.1017/CBO9781139644167
3. G.F. Sterman, *An Introduction to Quantum Field Theory* (Cambridge University Press, Cambridge, 1993)
4. Particle Data Group, R.L. Workman et al. (2022) Review of particle physics, PTEP **2022**, 083C01. https://doi.org/10.1093/ptep/ptac097
5. D. Pocanic, E. Frlez, A. van der Schaaf, Experimental study of rare charged pion decays. J. Phys. G **41**, 114002 (2014). https://doi.org/10.1088/0954-3899/41/11/114002. arXiv:1407.2865 [hep-ex]
6. A. Abashian et al., Angular Distributions of Positrons from pi+-mu+-e+ decays observed in a liquid hydrogen bubble chamber. Phys. Rev. **105**, 1927–1928 (1957). https://doi.org/10.1103/PhysRev.105.1927
7. S. Taylor, E.L. Koller, T. Huetter, P. Stamer, J. Grauman, Search for anomalous π^+ decay among τ^+ decay secondaries. Phys. Rev. Lett. **14**, 745–746 (1965). https://doi.org/10.1103/PhysRevLett.14.745
8. E. Frota-Pessoa, Isotropy in pi-minus mu decays. Phys. Rev. **177**, 2368–2370 (1969). https://doi.org/10.1103/PhysRev.177.2368
9. H. Hulubei, J. S. Auslander, E. M. Friedlander, S. Titeica, Angular distribution of muons in pi–mu decay at rest. Phys. Rev. **129**, 2789–2801 (1963). [Erratum: Phys. Rev. 131, 2841 (1963)]. https://doi.org/10.1103/PhysRev.131.2841
10. MINOS, P. Adamson et al., Testing Lorentz invariance and CPT conservation with NuMI neutrinos in the MINOS near detector. Phys. Rev. Lett. **101**, 151601 (2008). https://doi.org/10.1103/PhysRevLett.101.151601
11. MINOS, P. Adamson et al., Search for Lorentz invariance and CPT violation with muon antineutrinos in the MINOS near detector. Phys. Rev. D **85**, 031101 (2012). https://doi.org/10.1103/PhysRevD.85.031101. arXiv:1201.2631 [hep-ex]
12. B. Altschul, Contributions to pion decay from Lorentz violation in the weak sector. Phys. Rev. D **88**, 076015 (2013). https://doi.org/10.1103/PhysRevD.88.076015. arXiv:1308.2602 [hep-ph]
13. B. Altschul, Neutrino beam constraints on flavor-diagonal Lorentz violation. Phys. Rev. D **87**(9), 096004 (2013). https://doi.org/10.1103/PhysRevD.87.096004. arXiv:1302.2598 [hep-ph]
14. J.P. Noordmans, K.K. Vos, Limits on Lorentz violation from charged-pion decay. Phys. Rev. D **89**(10), 101702 (2014). https://doi.org/10.1103/PhysRevD.89.101702. arXiv:1404.7629 [hep-ph]
15. J.S. Díaz, A. Kostelecký, R. Lehnert, Relativity violations and beta decay. Phys. Rev. D **88**(7), 071902 (2013). https://doi.org/10.1103/PhysRevD.88.071902. arXiv:1305.4636 [hep-ph]
16. J.P. Noordmans, H.W. Wilschut, R.G.E. Timmermans, Limits on Lorentz violation from forbidden β decays. Phys. Rev. Lett. **111**(17), 171601 (2013). https://doi.org/10.1103/PhysRevLett.111.171601. arXiv:1308.5570 [hep-ph]
17. R. Fayyazuddin, *A Modern Introduction To Particle Physics*, 3rd edn. (Oxford University Press, Oxford, 2011). https://doi.org/10.1142/8064
18. V. D. Barger, R. J. N. Phillips, COLLIDER PHYSICS

---

[14] Another example would be from the $J = 0$ result in Eq. (39), when $E_a + E_b$ is getting on shell: $E_a + E_b \to M_W$. Because of the propagator denominator from N_{ab}, the transition of the $J = 0$ mode to zero occurs in exactly the same way as with the pion decay amplitude here.

19. N. Nakanishi, T*-product and false nonconservation of angular momentum in the pion decay. Mod. Phys. Lett. A **17**, 89–93 (2002). https://doi.org/10.1142/S0217732302006217

20. M. Jacob, G.C. Wick, On the general theory of collisions for particles with spin. Ann. Phys. **7**, 404–428 (1959). https://doi.org/10.1016/0003-4916(59)90051-X

21. W.M. Gibson, B.R. Pollard, *Symmetry Principles in Elementary Particle Physics* (Cambridge University Press, Cambridge, 2011)

22. E. Leader, *Spin in Particle Physics*, vol. 15 (Cambridge University Press, Cambridge, 2001)

23. D.H. Perkins, *Introduction to High Energy Physics*, 4th edn. (Cambridge University Press, Cambridge, 2000)

24. UA1, G. Arnison et al., Recent results on intermediate vector Boson properties at the CERN super proton synchrotron collider, Phys. Lett. B **166**, 484–490 (1986). https://doi.org/10.1016/0370-2693(86)91603-5

25. UA1, G. Arnison et al., Intermediate vector Boson properties at the CERN super proton synchrotron collider, EPL **1**, 327–345 (1986). https://doi.org/10.1209/0295-5075/1/7/002

26. UA1, C. Albajar et al., Studies of intermediate vector boson production and decay in UA1 at the CERN proton—antiproton collider. Z. Phys. C **44**, 15–61 (1989). https://doi.org/10.1007/BF01548582

27. D0, B. Abbott et al., Measurement of the angular distribution of electrons from $W \rightarrow e\nu$ decays observed in $p\bar{p}$ collisions at $\sqrt{s} = 1.8$ TeV. Phys. Rev. D **63**, 072001 (2001). https://doi.org/10.1103/PhysRevD.63.072001. arXiv:hep-ex/0009034

28. CDF, D. Acosta et al., Measurement of the polar-angle distribution of leptons from W boson decay as a function of the W transverse momentum in $p\bar{p}$ collisions at $\sqrt{s} = 1.8$ TeV, Phys. Rev. D **70**, 032004 (2004). https://doi.org/10.1103/PhysRevD.70.032004. arXiv:hep-ex/0311050

29. ATLAS, G. Aad et al., Measurement of the inclusive $W^{\pm}$ and Z/gamma cross sections in the electron and muon decay channels in pp collisions at $\sqrt{s} = 7$ TeV with the ATLAS detector. Phys. Rev. D **85**, 072004 (2012). https://doi.org/10.1103/PhysRevD.85.072004. arXiv:1109.5141 [hep-ex]

30. CMS, A. M. Sirunyan et al., Measurements of the W boson rapidity, helicity, double-differential cross sections, and charge asymmetry in pp collisions at $\sqrt{s} = 13$ TeV. Phys. Rev. D **102**(9), 092012 (2020). https://doi.org/10.1103/PhysRevD.102.092012. arXiv:2008.04174 [hep-ex]

31. D0, V. M. Abazov et al., Evidence for S-Channel Single Top Quark Production in $p\bar{p}$ Collisions at $\sqrt{s} = 1.96$ TeV. Phys. Lett. B **726**, 656–664 (2013). https://doi.org/10.1016/j.physletb.2013.09.048. arXiv:1307.0731 [hep-ex]

32. CDF, D0, T. A. Aaltonen et al., Observation of s-channel production of single top quarks at the Tevatron. Phys. Rev. Lett. **112**, 231803 (2014). https://doi.org/10.1103/PhysRevLett.112.231803. arXiv:1402.5126 [hep-ex]

33. ATLAS, G. Aad et al., Evidence for single top-quark production in the *s*-channel in proton-proton collisions at $\sqrt{s} = 8$ TeV with the ATLAS detector using the matrix element method. Phys. Lett. B **756**, 228–246 (2016). https://doi.org/10.1016/j.physletb.2016.03.017. arXiv:1511.05980 [hep-ex]

34. CMS, V. Khachatryan et al., Search for s channel single top quark production in pp collisions at $\sqrt{s} = 7$ and 8 TeV. JHEP **09**, 027 (2016). https://doi.org/10.1007/JHEP09(2016)027. arXiv:1603.02555 [hep-ex]